SUPPLEMENTARY INFORMATION

Chloroacetamide Fragment Library Screening Identifies New Scaffolds for Covalent Inhibition of the TEAD•YAP1 Interaction

Khuchtumur Bum-Erdene[1], Mona K. Ghozayel[1], Mark Zhang[1], Giovanni Gonzalez-Gutierrez[2] and Samy O. Meroueh[1]*

[1]Department of Biochemistry and Molecular Biology, Indiana University School of Medicine, Indianapolis, Indiana, 46202

*Corresponding author

Corresponding Author and Lead Contact:

Samy O. Meroueh

Department of Biochemistry and Molecular Biology

Indiana University School of Medicine

635 Barnhill drive, MS4021, Indianapolis, IN 46202

Tel: (317) 274-8315

Fax: (317) 278-9217

E-mail: smeroueh@iu.edu

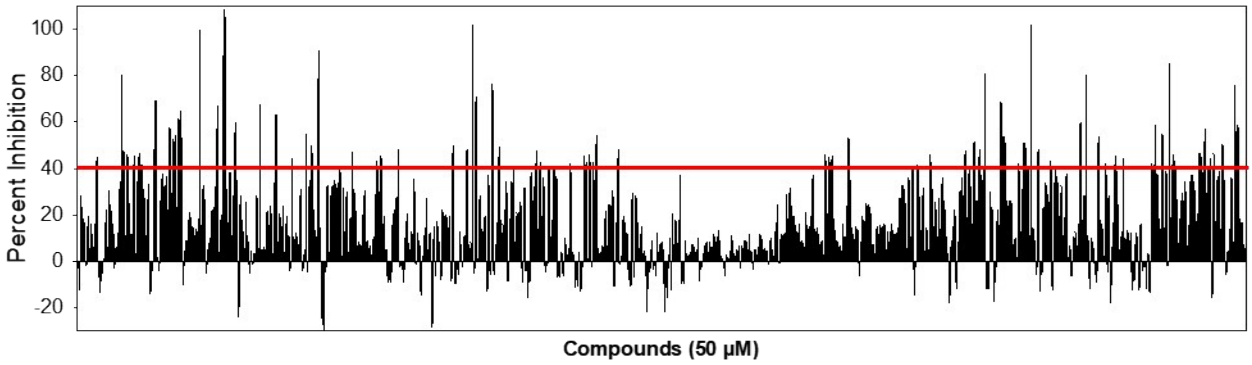

Figure S1. A total 658 chloroacetamide fragments and compounds were screened to identify TEAD4•YAP1 interaction inhibitors. TEAD4 (64 nM) was incubated with fragments and compounds at 50 µM concentration for 24 h at 4°C prior to binding detection by polarization using fluorescently labeled $YAP1_{60-99}$ peptide (n=2). The red line was drawn to highlight the 40% threshold that was used to select candidates for follow-up studies.

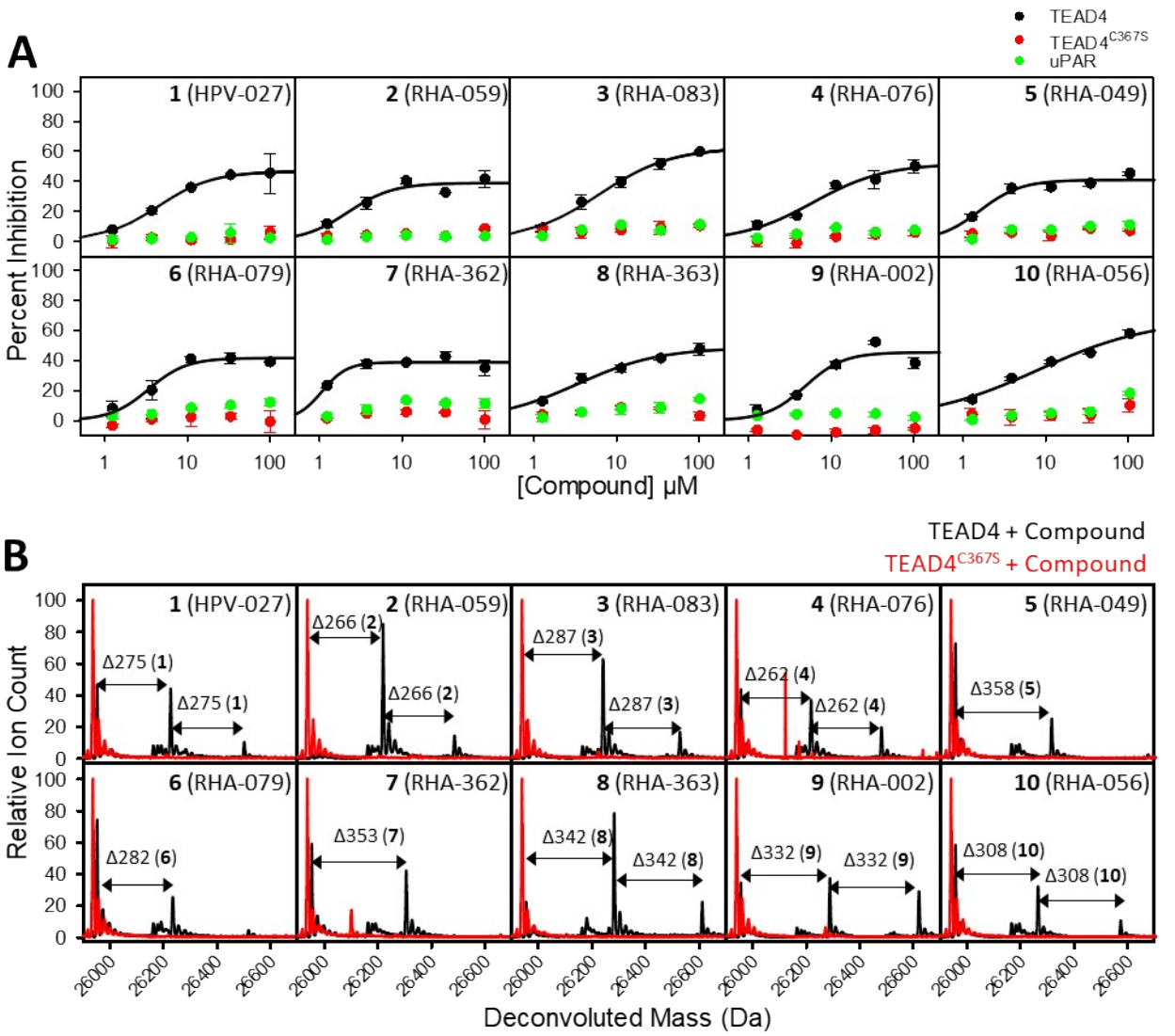

Figure S2. (A) Inhibition of TEAD4, TEAD4^{C367S} and uPAR interactions by compounds using our FP assays after incubation of protein with compound for 24 h at 4°C (TEAD4 n=3; TEAD4^{C367S} and uPAR n=2). **(B)** Whole-protein mass spectrometry of TEAD4 and TEAD4^{C367S} mutant after 24 h 4 °C incubation with 100 µM compound. TEAD4 was detected at 25953 Da, TEAD4^{C367S} was detected at 25937 Da, and peaks for protein-compound adducts were also detected with a mass that matches the covalent complex following reaction of chloroacetamide with central pocket Cys-367 cysteine. In some cases, an additional peak was detected that corresponds to the protein in a covalent complex with two compounds likely due to reaction at another cysteine on the protein. These are depicted by the second peak in the red spectrum in each panel.

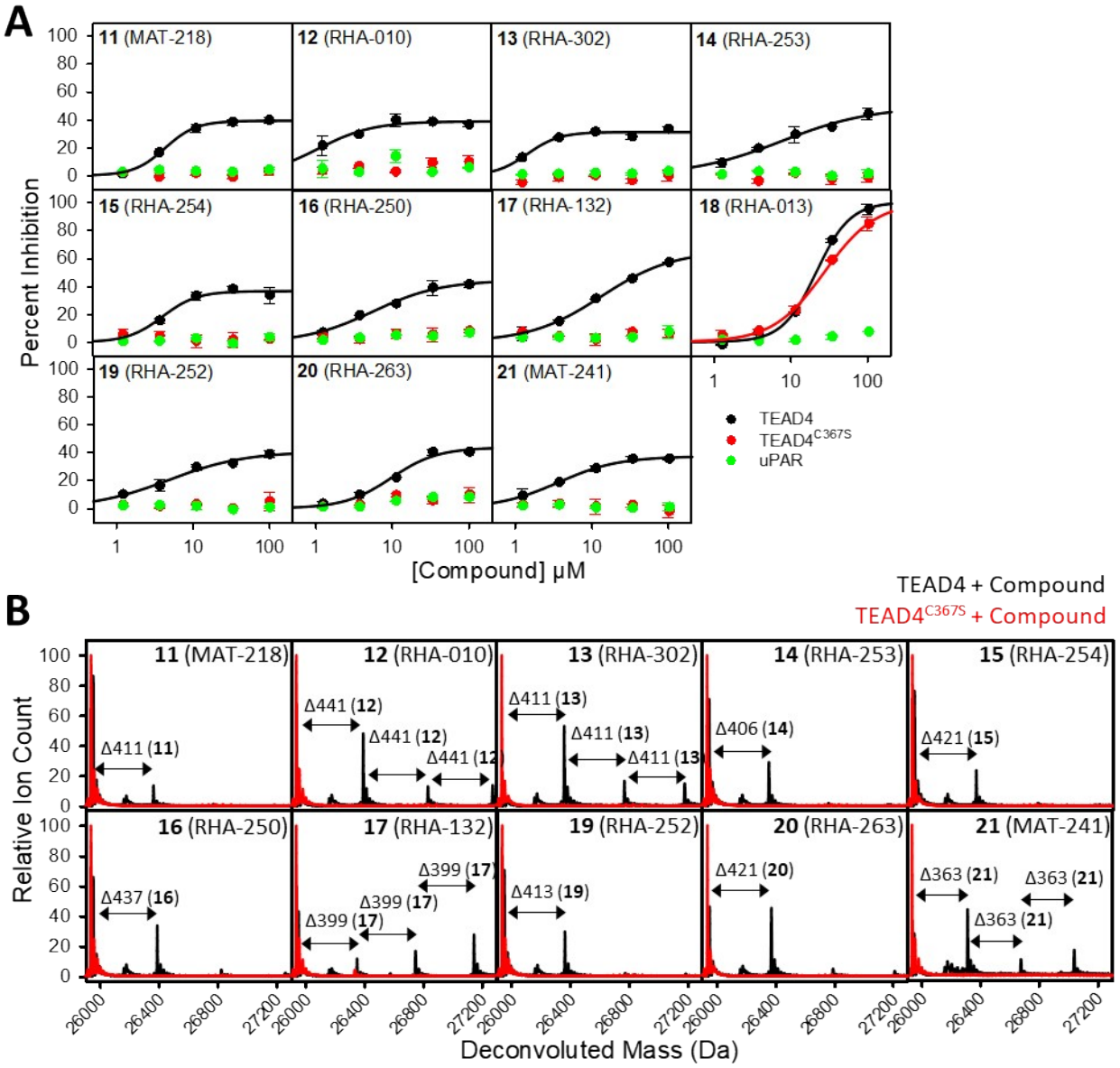

Figure S3. (A) Inhibition of TEAD4, TEAD4^{C367S} and uPAR interactions by compounds using our FP assays after incubation of protein with compound for 24 h at 4°C (TEAD4 n=3; TEAD4^{C367S} and uPAR n=2). **(B)** Whole-protein mass spectrometry of TEAD4 and TEAD4^{C367S} mutant after 24 h 4 °C incubation with 100 µM compound. TEAD4 was detected at 25953 Da, TEAD4^{C367S} was detected at 25937 Da, and peaks for protein-compound adducts were also detected with a mass that matches the covalent complex following reaction of chloroacetamide with central pocket Cys-367 cysteine. In some cases, additional peaks were detected that correspond to the protein in a covalent complex with two or three compounds likely due to reaction at another cysteine on the protein. These are depicted by the second peak in the red spectrum in each panel.

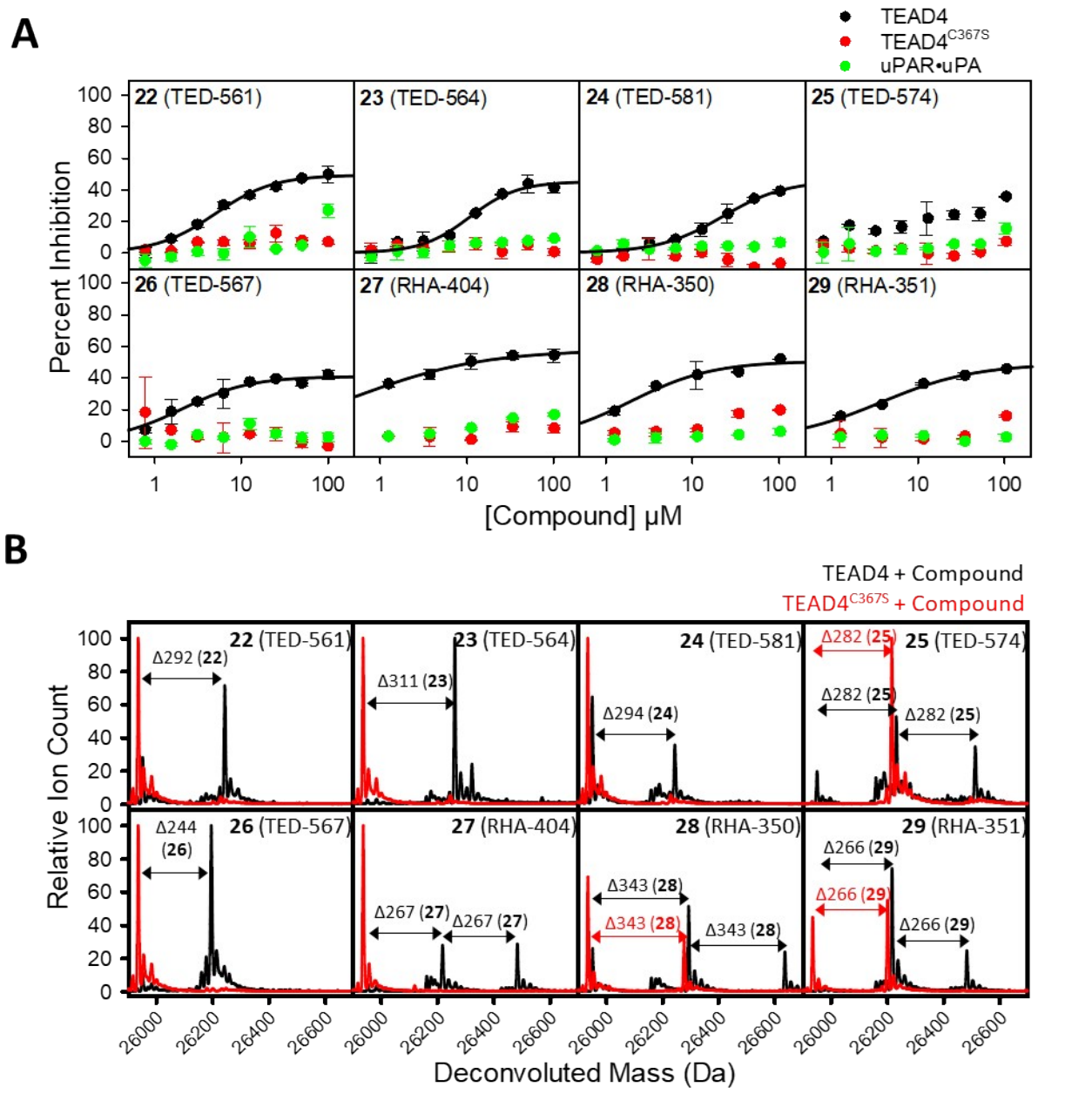

Figure S4. (A) Inhibition of TEAD4, TEAD4^{C367S} and uPAR interactions by compounds using our FP assays after incubation of protein with compound for 24 h at 4°C (TEAD4 n=3; TEAD4^{C367S} and uPAR n=2). **(B)** Whole-protein mass spectrometry of TEAD4 and TEAD4^{C367S} mutant after 24 h 4 °C incubation with 100 µM compound. TEAD4 was detected at 25953 Da, TEAD4^{C367S} was detected at 25937 Da, and peaks for protein-compound adducts were also detected with a mass that matches the covalent complex following reaction of chloroacetamide with central pocket Cys-367 cysteine. In some cases, an additional peak was detected that corresponds to the protein in a covalent complex with two compounds likely due to reaction at another cysteine on the protein. These are depicted by the second peak in the red spectrum in each panel.

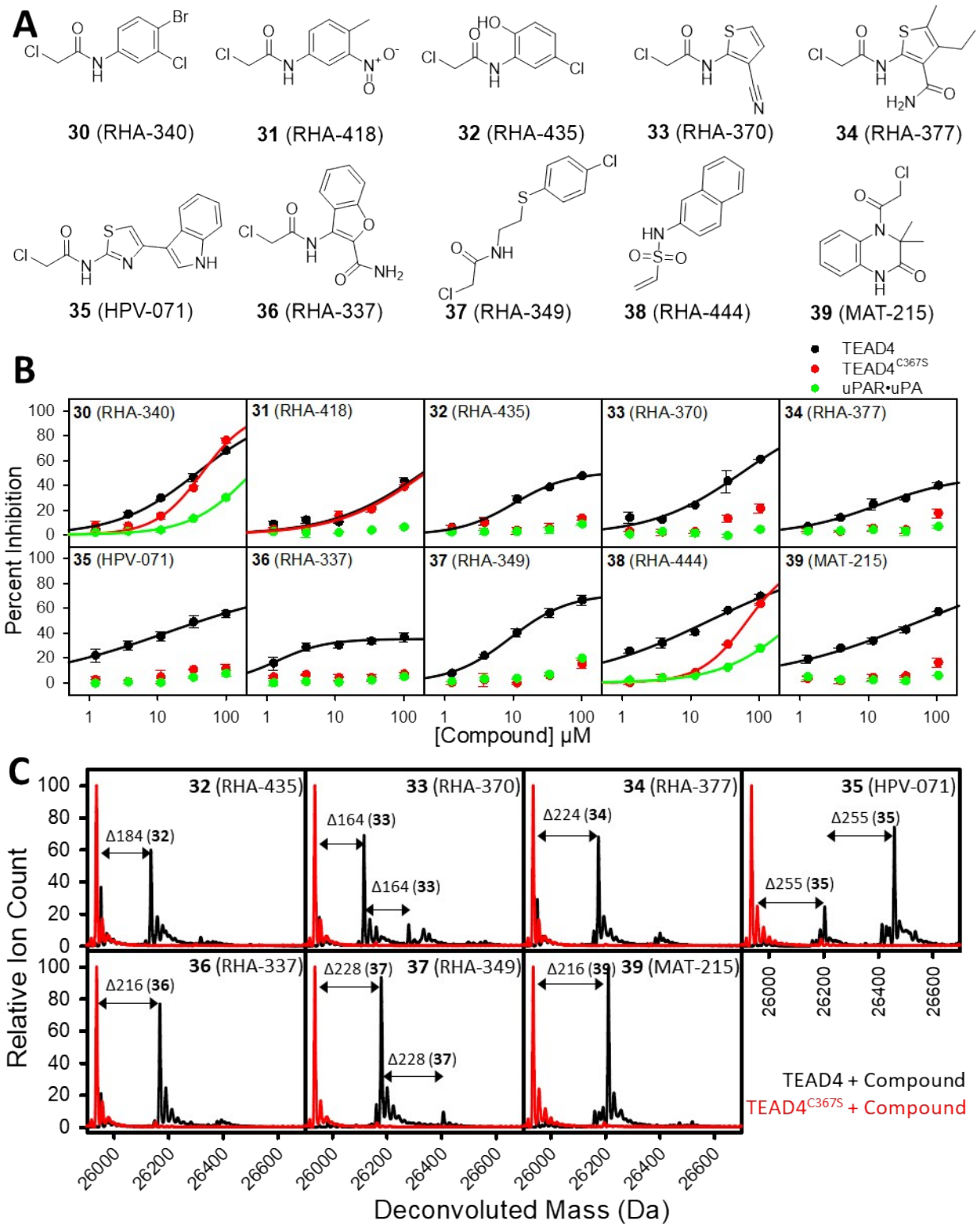
A
30 (RHA-340)
31 (RHA-418)
32 (RHA-435)
33 (RHA-370)
34 (RHA-377)
35 (HPV-071)
36 (RHA-337)
37 (RHA-349)
38 (RHA-444)
39 (MAT-215)
B
TEAD4
TEAD4C367S
uPAR•uPA
Percent Inhibition
[Compound] µM
C
Relative Ion Count
Δ184 (32)
Δ164 (33)
Δ224 (34)
Δ255 (35)
Δ216 (36)
Δ228 (37)
Δ216 (39)
TEAD4 + Compound
TEAD4C367S + Compound
Deconvoluted Mass (Da)

D

Compound	TEAD4 Mass Adduct (%)	TEAD4 WT IC_{50} at 24 h (μM)	TEAD4^{C367S} IC_{50} at 24 h (μM)	uPAR•AE-147 IC_{50} at 24 h (μM)
30 (RHA-340)	ND	38.0 ± 3.8, max 100%	44.8 ± 3.1	242 ± 67.5
31 (RHA-418)	ND	170 ± 60.1, max 100%	207 ± 57.5	NI
32 (RHA-435)	61	10.3 ± 3.8, max 49%	NI	NI
33 (RHA-370)	70, 12	67.4 ± 12.1, max 100%	NI	NI
34 (RHA-377)	68	13.0 ± 9.4, max 48%	NI	NI
35 (HPV-071)	23, 77	3.5 ± 0.5, max 60%	NI	NI
36 (RHA-337)	79	1.4 ± 0.3, max 35%	NI	NI
37 (RHA-349)	91, 9	8.3 ± 0.8, max 73%	NI	NI
38 (RHA-444)	ND	20.9 ± 14.8, max 100%	50.2 ± 20.4	285 ± 183
39 (MAT-215)	100	5.6 ± 8.1, max 100%	NI	NI

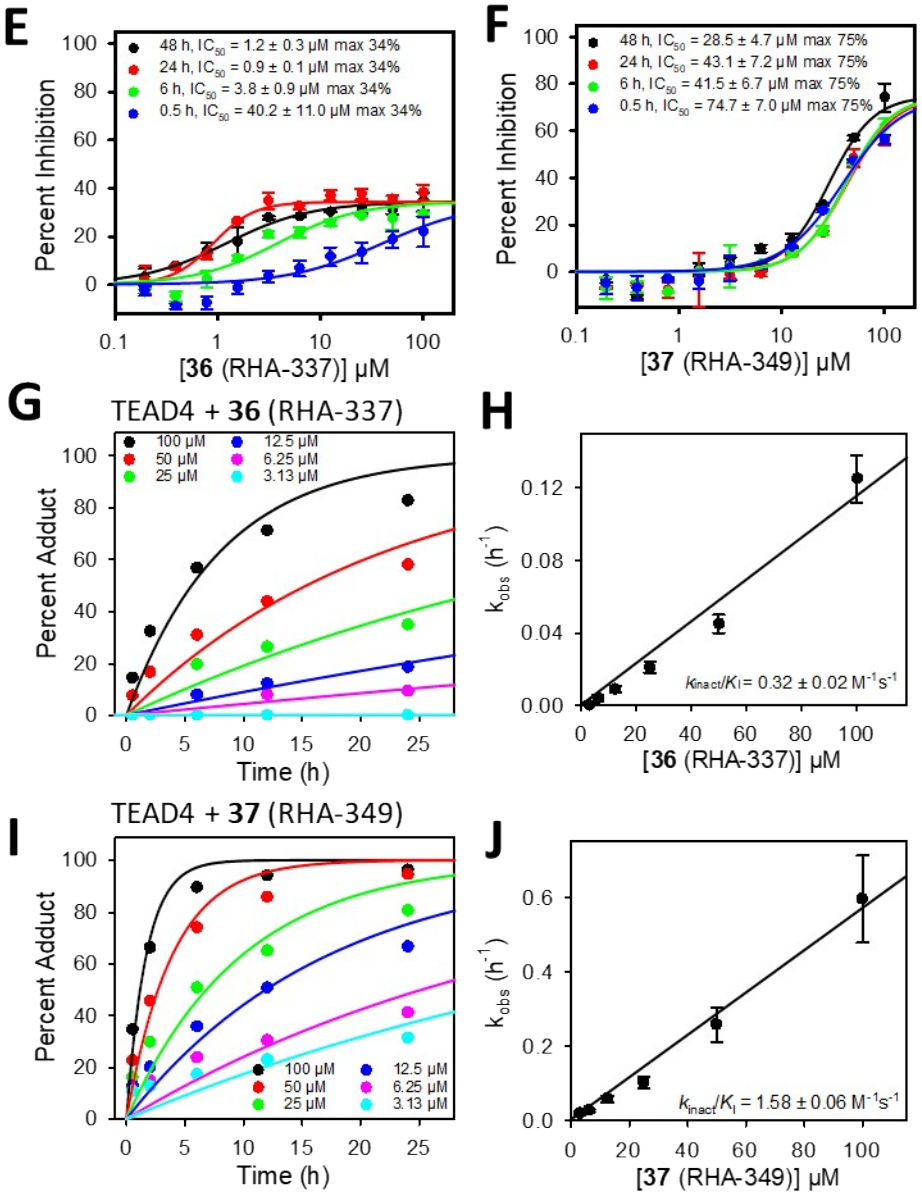

Figure S5. (A) Chemical structure of ten fragments that inhibit the TEAD4•YAP1 interaction. **(B)** Inhibition of TEAD4, TEAD4^{C367S} and uPAR interactions by compounds using our FP assays after incubation of

protein with compound for 24 h at 4°C (TEAD4 n=3; TEAD4^{C367S} and uPAR n=2). **(C)** Whole-protein mass spectrometry of TEAD4 and TEAD4^{C367S} mutant after 24 h 4 °C incubation with 100 μM compound. TEAD4 was detected at 25953 Da, TEAD4^{C367S} was detected at 25937 Da, and peaks for protein-compound adducts were also detected with a mass that matches the covalent complex following reaction of chloroacetamide with central pocket Cys-367 cysteine. In some cases, an additional peak was detected that corresponds to the protein in a covalent complex with two compounds likely due to reaction at another cysteine on the protein. These are depicted by the second peak in the red spectrum in each panel. **(D)** Table of IC_{50}s for inhibition of TEAD4 binding to YAP1 after 24 h incubation at 4°C with TEAD4, TEAD4^{C367S} and uPAR. **(E)** TEAD4 was incubated with various concentrations of **36** (RHA-337) and times over a 0.5-48 h period at 4°C prior to detection of binding to fluorescently labeled $YAP1_{60-99}$ peptide (n=2). **(F)** TEAD4 was incubated with various concentrations of **37** (RHA-349) and times over a 0.5-48 h period at 4°C prior to detection of binding to fluorescently labeled $YAP1_{60-99}$ peptide (n=2). **(G)** TEAD4 was incubated with various concentrations of **36** (RHA-337) and times over a 0.5-24 h period at 4°C. The reactions were quenched with 0.1 M formic acid and adduct formation was quantified by whole-protein mass spectrometry. Rate constant, k_{obs}, for each concentration of fragment was determined by fitting an exponential function. **(H)** Rate constant, k_{obs}, versus concentration of **36** (RHA-337) was fit with a linear function to determine k_{inact}/K_I. **(I)** TEAD4 was incubated with various concentrations of **37** (RHA-349) and times over a 0.5-24 h period at 4°C. The reactions were quenched with 0.1 M formic acid and adduct formation was quantified by whole-protein mass spectrometry. Rate constant, k_{obs}, for each concentration of fragment was determined by fitting an exponential function. **(J)** Rate constant, k_{obs}, versus concentration of **37** (RHA-349) was fit with a linear function to determine k_{inact}/K_I.

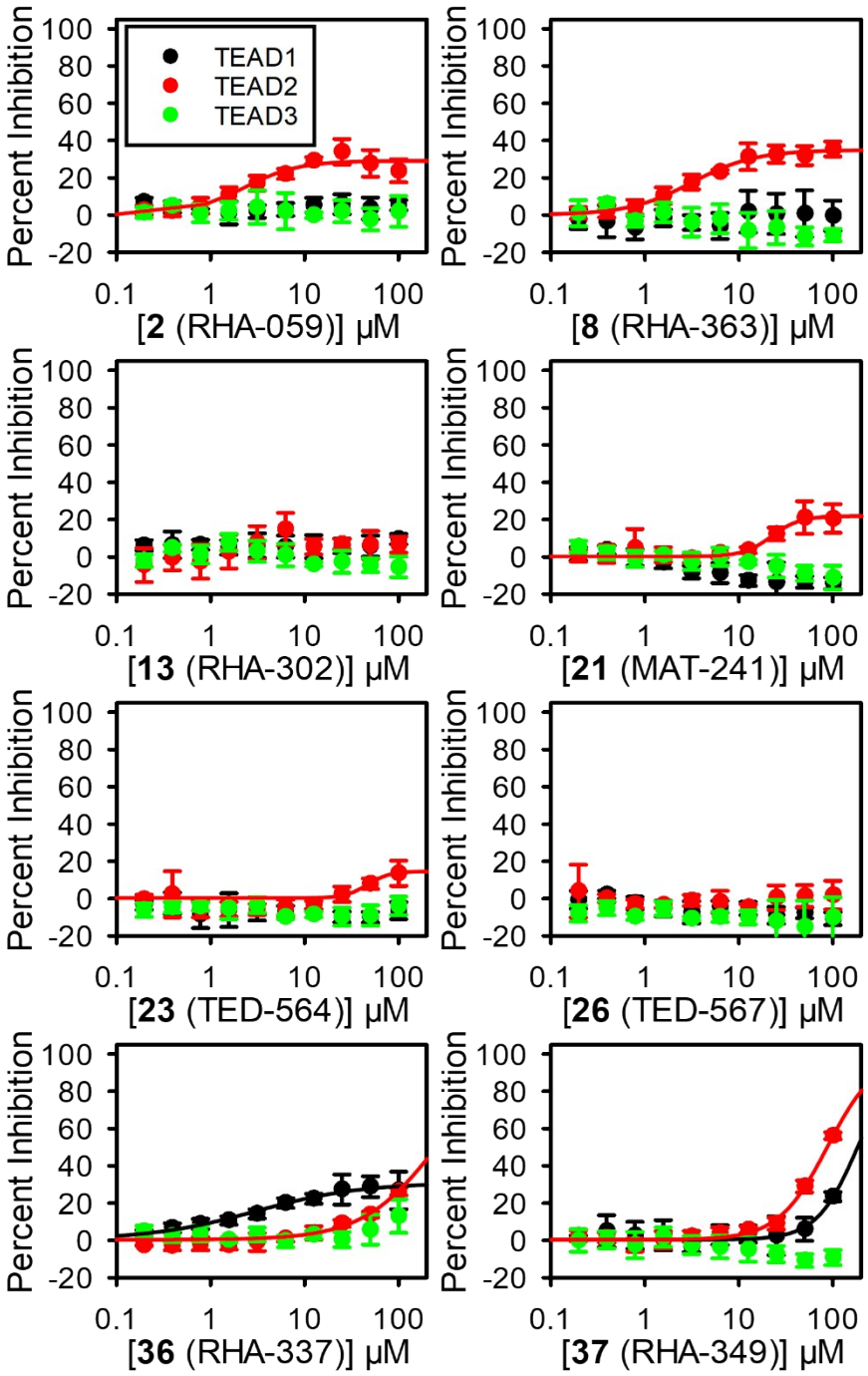

Figure S6. Inhibition of TEAD1-3 binding to fluorescently labeled YAP1 peptide**.** TEAD1-3 were incubated with varying concentrations of compounds for 24 h at 4°C prior to detection of binding to fluorescently labeled $YAP1_{60-99}$ peptide (n=3).

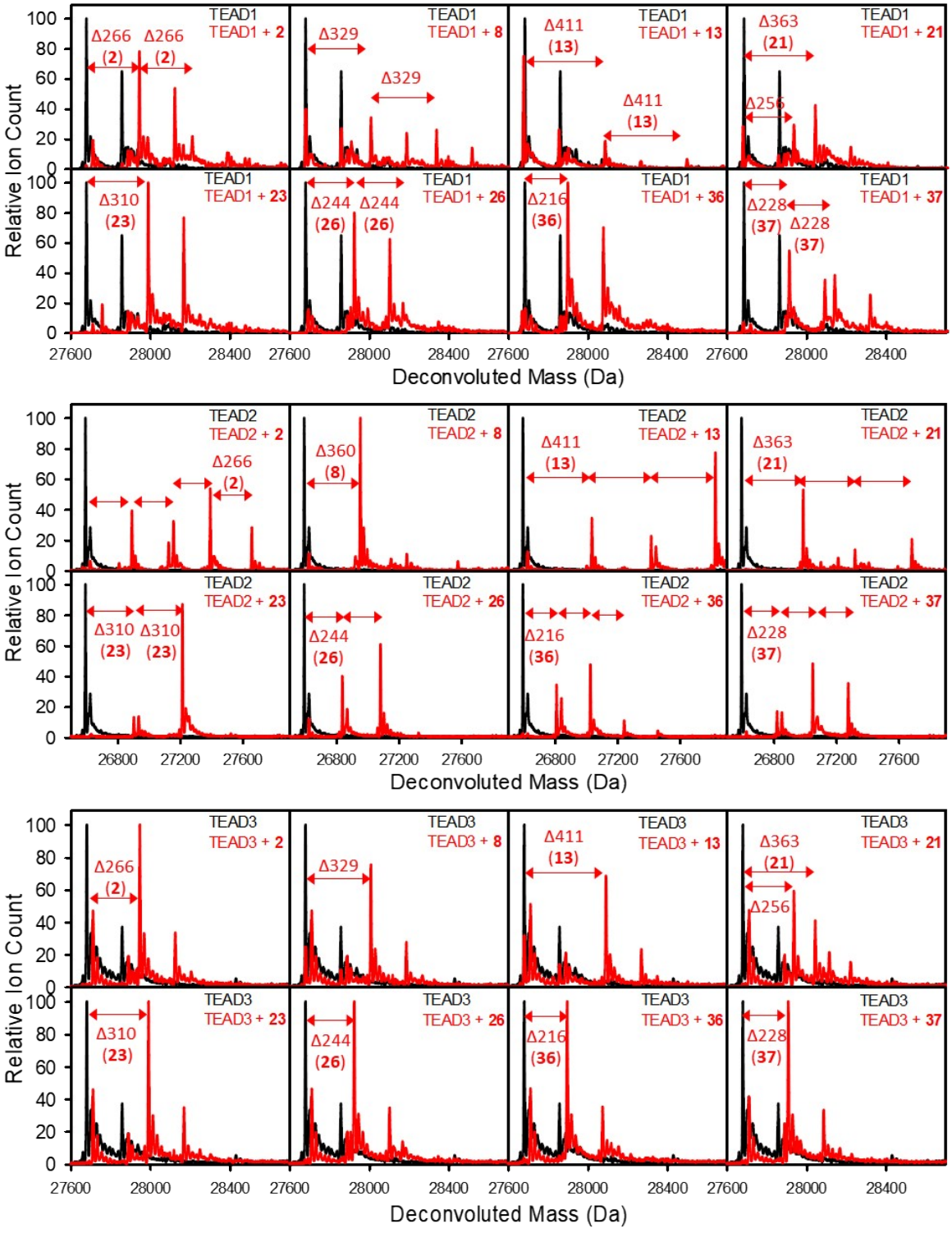

Figure S7. Reaction of compounds with TEAD1-3. Whole-protein mass spectrometry of TEAD1, TEAD2 and TEAD3 after 24 h 4°C incubation with 100 µM compound. The extent of adduct formation with TEAD1-3 for each compound is listed in **Table S1**. **(A)** TEAD1 incubated with DMSO resulted in two peaks at 27679 and 27857 Da. The second peak at 27857 Da corresponds to N-terminal gluconoylation of TEAD1. Compound adducts to TEAD1 were detected at mass differences equal to the molecular weight the compound with loss of chlorine and hydrogen. Compound **8** (RHA-363) formed a 329 Da adduct to TEAD1

instead of the expected 360 Da. Compound **21** (MAT-241) formed an extra peak with an adduct size of 256 Da. **(B)** TEAD2 incubated with DMSO was found at 26594 Da and peaks for protein-compound adducts were also detected with a mass that matches the covalent complex following reaction of chloroacetamide **(C)** TEAD3 incubated with DMSO resulted in two peaks at 27682 and 27860 Da. The second peak at 27860 Da was an N-terminal gluconoylation of TEAD3. Peaks for protein-compound adducts were also detected with a mass that matches the covalent complex following reaction of chloroacetamide. Compound **8** (RHA-363) formed a 329 Da adduct to TEAD3 instead of the expected 360 Da. Compound **21** (MAT-214) formed an extra peak with an adduct size of 256 Da.

Table S1. Whole-Protein Mass Spectrometry of TEAD1-3 Incubated with 100 µM Compound at 4°C

	Compound Adduct at 24 h 4°C (%)		
Compound	**TEAD1**	**TEAD2**	**TEAD3**
2 (RHA-059)	80, 20 [a]	0, 18, 54, 28	100
8 (RHA-363)	35 [b], 24 [b]	100	75 [b]
13 (RHA-302)	18, 7	0, 23, 77	68
21 (MAT-241)	29 [c], 42	61, 16, 23	59 [c], 41
23 (TED-564)	100	13, 87	100
26 (TED-567)	80, 20	39, 61	100
36 (RHA-337)	100	37, 51, 12	100
37 (RHA-349)	56, 38	17, 48, 35	100

[a] Additional protein-compound adduct detected in the mass spectrum

[b] Compound **8** (RHA-363) adduct to TEAD1 and TEAD3 was 329 Da instead of the expected 360 Da.

[c] Compound **21** (MAT-241) formed an additional 256 Da adduct to TEAD1 and TEAD3.

Covalent Inhibitors

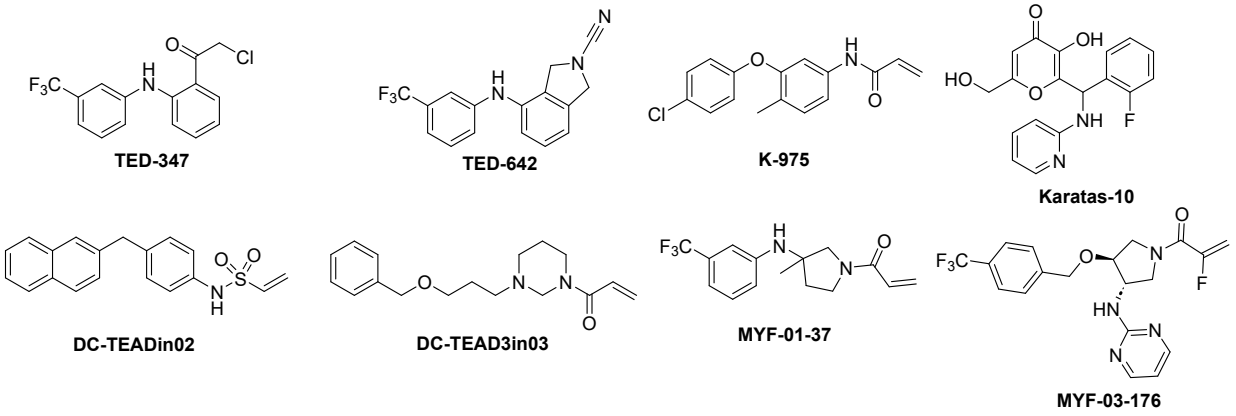

Non-covalent Inhibitors

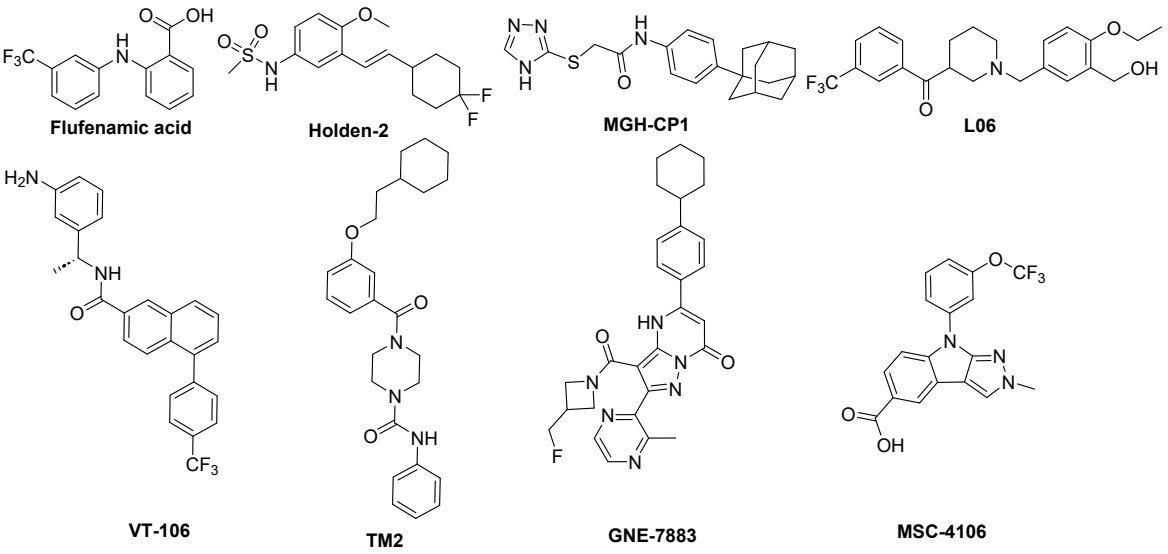

Figure S8. Chemical structures of covalent and non-covalent inhibitors of TEAD palmitate pocket. Covalent inhibitors: TED-347 [1], TED-642 [2], K-975 [3], Karatas-10 [4], DC-TEADin02 [5], DC-TEAD3in03 [6], MYF-01-37 [7], MYF-03-176 [8]. Non-covalent inhibitors: Flufenamic acid [9], Holden-2 [10], MGH-CP1 [11, 12], L06 [13], VT-106 [14], TM2 [15], GNE-7883 [16], MSC-4106 [17].

REFERENCES

1. K. Bum-Erdene, D. Zhou, G. Gonzalez-Gutierrez, M. K. Ghozayel, Y. Si, D. Xu, H. E. Shannon, B. J. Bailey, T. W. Corson, K. E. Pollok, C. D. Wells and S. O. Meroueh, *Cell Chem Biol*, 2019, **26**, 378-389 e313.
2. K. Bum-Erdene, I. J. Yeh, G. Gonzalez-Gutierrez, M. K. Ghozayel, K. Pollok and S. O. Meroueh, *J Med Chem*, 2023, **66**, 266-284.
3. A. Kaneda, T. Seike, T. Danjo, T. Nakajima, N. Otsubo, D. Yamaguchi, Y. Tsuji, K. Hamaguchi, M. Yasunaga, Y. Nishiya, M. Suzuki, J. I. Saito, R. Yatsunami, S. Nakamura, Y. Sekido and K. Mori, *Am J Cancer Res*, 2020, **10**, 4399-4415.
4. H. Karatas, M. Akbarzadeh, H. Adihou, G. Hahne, A. V. Pobbati, E. Yihui Ng, S. M. Guéret, S. Sievers, A. Pahl, M. Metz, S. Zinken, L. Dötsch, C. Nowak, S. Thavam, A. Friese, C. Kang, W. Hong and H. Waldmann, *Journal of Medicinal Chemistry*, 2020, **63**, 11972-11989.
5. W. Lu, J. Wang, Y. Li, H. Tao, H. Xiong, F. Lian, J. Gao, H. Ma, T. Lu, D. Zhang, X. Ye, H. Ding, L. Yue, Y. Zhang, H. Tang, N. Zhang, Y. Yang, H. Jiang, K. Chen, B. Zhou and C. Luo, *European Journal of Medicinal Chemistry*, 2019, **184**, 111767.
6. T. Lu, Y. Li, W. Lu, T. Spitters, X. Fang, J. Wang, S. Cai, J. Gao, Y. Zhou, Z. Duan, H. Xiong, L. Liu, Q. Li, H. Jiang, K. Chen, H. Zhou, H. Lin, H. Feng, B. Zhou, C. L. Antos and C. Luo, *Acta Pharmaceutica Sinica B*, 2021, **11**, 3206-3219.
7. M. Fan, W. Lu, J. Che, N. P. Kwiatkowski, Y. Gao, H.-S. Seo, S. B. Ficarro, P. C. Gokhale, Y. Liu, E. A. Geffken, J. Lakhani, K. Song, M. Kuljanin, W. Ji, J. Jiang, Z. He, J. Tse, A. S. Boghossian, M. G. Rees, M. M. Ronan, J. A. Roth, J. D. Mancias, J. A. Marto, S. Dhe-Paganon, T. Zhang and N. S. Gray, *eLife*, 2022, **11**, e78810.
8. W. Lu, M. Fan, W. Ji, J. Tse, I. You, S. B. Ficarro, I. Tavares, J. Che, A. Y. Kim, X. Zhu, A. Boghossian, M. G. Rees, M. M. Ronan, J. A. Roth, S. M. Hinshaw, B. Nabet, S. M. Corsello, N. Kwiatkowski, J. A. Marto, T. Zhang and N. S. Gray, *Journal of Medicinal Chemistry*, 2023, **66**, 4617-4632.
9. Ajaybabu V. Pobbati, X. Han, Alvin W. Hung, S. Weiguang, N. Huda, G.-Y. Chen, C. Kang, Cheng San B. Chia, X. Luo, W. Hong and A. Poulsen, *Structure*, 2015, **23**, 2076-2086.
10. J. K. Holden, J. J. Crawford, C. L. Noland, S. Schmidt, J. R. Zbieg, J. A. Lacap, R. Zang, G. M. Miller, Y. Zhang, P. Beroza, R. Reja, W. Lee, J. Y. K. Tom, R. Fong, M. Steffek, S. Clausen, T. J. Hagenbeek, T. Hu, Z. Zhou, H. C. Shen and C. N. Cunningham, *Cell Rep*, 2020, **31**, 107809.
11. Q. Li, Y. Sun, G. K. Jarugumilli, S. Liu, K. Dang, J. L. Cotton, J. Xiol, P. Y. Chan, M. DeRan, L. Ma, R. Li, L. J. Zhu, J. H. Li, A. B. Leiter, Y. T. Ip, F. D. Camargo, X. Luo, R. L. Johnson, X. Wu and J. Mao, *Cell Stem Cell*, 2020, **26**, 675-692.e678.
12. Y. Sun, L. Hu, Z. Tao, G. K. Jarugumilli, H. Erb, A. Singh, Q. Li, J. L. Cotton, P. Greninger, R. K. Egan, Y. Tony Ip, C. H. Benes, J. Che, J. Mao and X. Wu, *Nature Communications*, 2022, **13**, 6744.
13. L. Li, R. Li and Y. Wang, *Bioorganic Chemistry*, 2022, **122**, 105707.
14. T. T. Tang, A. W. Konradi, Y. Feng, X. Peng, M. Ma, J. Li, F.-X. Yu, K.-L. Guan and L. Post, *Molecular Cancer Therapeutics*, 2021, **20**, 986-998.
15. L. Hu, Y. Sun, S. Liu, H. Erb, A. Singh, J. Mao, X. Luo and X. Wu, *eLife*, 2022, **11**, e80210.
16. T. J. Hagenbeek, J. R. Zbieg, M. Hafner, R. Mroue, J. A. Lacap, N. M. Sodir, C. L. Noland, S. Afghani, A. Kishore, K. P. Bhat, X. Yao, S. Schmidt, S. Clausen, M. Steffek, W. Lee, P. Beroza, S. Martin, E. Lin, R. Fong, P. Di Lello, M. H. Kubala, M. N. Y. Yang, J. T. Lau, E. Chan, A. Arrazate, L. An, E. Levy, M. N. Lorenzo, H.-J. Lee, T. H. Pham, Z. Modrusan, R. Zang, Y.-C. Chen, M. Kabza, M. Ahmed, J. Li, M. T. Chang, D. Maddalo, M. Evangelista, X. Ye, J. J. Crawford and A. Dey, *Nature Cancer*, 2023, **4**, 812-828.
17. T. Heinrich, C. Peterson, R. Schneider, S. Garg, D. Schwarz, J. Gunera, A. Seshire, L. Kötzner, S. Schlesiger, D. Musil, H. Schilke, B. Doerfel, P. Diehl, P. Böpple, A. R. Lemos, P. M. F. Sousa, F.

Freire, T. M. Bandeiras, E. Carswell, N. Pearson, S. Sirohi, M. Hooker, E. Trivier, R. Broome, A. Balsiger, A. Crowden, C. Dillon and D. Wienke, *Journal of Medicinal Chemistry*, 2022, **65**, 9206-9229.